Bond-order potential and cluster recursion for the description of chemical bonds: Efficient real-space methods for tight-binding molecular dynamics

A. P. Horsfield, A. M. Bratkovsky, D. G. Pettifor, and M. Aoki*
Oxford University, Department of Materials, Parks Road, Oxford OX1 3PH, United Kingdom
(Received 7 August 1995)

The tight-binding model is presented as a successful theory for describing cohesion. It allows for rapid, but accurate, evaluation of electronic properties, total energies, and forces, while being simple enough to allow insight into the nature of bonding. The problem of applying this model to very large systems by diagonalizing the Hamiltonian matrix is discussed. Moments methods provide an efficient way to evaluate energies and forces from the Hamiltonian, even for large systems. However, for systems with sharp features in a broad density of states, many moments are required to achieve convergence. By reference to a moments method [the bond-order potential (BOP)] and a cluster-based method [cluster recursion (CR)], the origin of the need for many moments is explained. In particular, it is found that the inclusion of an *exact* description of the first-neighbor shell is important for obtaining accurate forces. For strongly covalent systems it also improves the energy convergence. Whereas CR gives rapid convergence with respect to number of levels, BOP is found to give more rapid convergence with respect to CPU time.

I. INTRODUCTION

Widespread interest in the atomistic modeling of materials properties is being shown at the moment, with many methods presently available, different ones being applicable to different problems. There is considerable effort being made to find new methods that are applicable to a wide range of materials but which are also computationally efficient. *Ideally* a single method (or a set of compatible methods that can be used together in a systematic way) that can be applied to all systems will be found since many interesting problems (such as catalysis) involve several materials with quite different properties. At present no such complete scheme exists, though considerable progress towards it has been made.

To reach this goal, we need a single general underlying theory of cohesion, and one or more appropriate numerical techniques to implement the theory. To be general, the underlying theory has to be based on a quantum mechanical description of electron motion, since the differences in materials properties lie in the differences in the electronic structure for the materials. For instance, metallic systems have wave functions that must be viewed as long ranged, whereas strongly covalent systems can be characterized by short-ranged wave functions (leading to the concept of the chemical bond).

There are a number of quantum mechanical methods that are routinely used ranging from very accurate many-electron *ab initio* methods such as quantum Monte Carlo, through slightly less accurate single electron *ab initio* methods such as the local-density approximation (LDA) to density-functional theory,[1] down to the semiempirical methods such as tight binding (TB).[2,3] It is now becoming apparent that TB schemes can offer sufficient accuracy for many materials as well as great simplicity in computation and analysis of results. They have been applied successfully to metallic systems,[4–6] semiconducting systems,[7–14] including the liquid phase,[15–18] and strongly covalent systems.[19,20] Thus TB provides a good general theory of cohesion for computer modeling, though it cannot yet claim to be universal in its applicability.

The appropriate numerical technique for implementing TB when only a small number of atoms is being considered is direct diagonalization of the Hamiltonian matrix. However, for this method, the time per molecular dynamics (MD) step scales as the third power of the number of atoms in the unit cell. This scaling is disastrous for simulations of large numbers of atoms: it sets a practical limit of order 100 atoms for MD. Thus it is necessary to find methods that can extract the useful information from the Hamiltonian matrix (such as the total band-structure energy and the contribution of the band-structure energy to the forces on the atoms) with a much better scaling, ideally linear scaling [$O(N)$ methods].

Several $O(N)$ methods suitable for TB have been proposed recently. In this paper we are interested in the *moments based methods*.[21–26] We focus on these methods since they have been successful for describing electronic structure, and for molecular dynamics (MD), and often allow insight into the nature of bonding. Traditionally these methods have been designed to be used with only a few moments (up to about 11). However, it has been found that for MD for certain systems many moments are necessary in order to reach convergence. In this paper we aim to shed light on the origin of this need, and to spell out the correct way to handle the many moments. We do this by comparing *one* moments-based method (the bond-order potential[23,24]) with a cluster-based method, which is explained below. However, the conclusions apply to moments methods in general.

In the remainder of this paper we outline the TB model, with some details about the density matrix and Green's functions. The central ideas behind moments methods are given, together with details of the bond-order potential. The cluster method is then described, and results for energies and forces from the two approaches are compared for a variety of systems.

II. TIGHT BINDING

It is convenient at this point to note some key concepts connected with the TB model of cohesion.[27,3] It will be assumed that the basis set is an orthonormal set of atomiclike orbitals $|i\alpha\rangle$ where i is a site index, and α is an orbital index. The Hamiltonian can then be represented by the matrix $H_{i\alpha,j\beta}=\langle i\alpha|\hat{H}|j\beta\rangle$. The on-site elements of the matrix are given the symbols: $\varepsilon_{i\alpha}=H_{i\alpha,i\alpha}$. The cohesive energy, assuming that the electrons are at a finite temperature T, is written as the sum of bond, promotion, entropic, and repulsive energies:

$$\begin{aligned}E_{coh}&=E_{bond}+E_{prom}+E_{rep}+E_{ent}\\&=2\sum_{i\alpha}\int(E-\varepsilon_{i\alpha})n_{i\alpha}(E)f[(E-\mu)/k_BT]dE\\&\quad+\sum_{i\alpha}\varepsilon_{i\alpha}(N_{i\alpha}-N^0_{i\alpha})+\frac{1}{2}\sum_{i\neq j}\phi(r_{ij})\\&\quad-2k_BT\sum_{i\alpha}\int\sigma[(E-\mu)/k_BT]n_{i\alpha}(E)dE,\end{aligned}\tag{1}$$

where $n_{i\alpha}(E)$ is the density of states projected onto orbital $|i\alpha\rangle$, $N_{i\alpha}$ and $N^0_{i\alpha}$ are the number of electrons in orbital $|i\alpha\rangle$ in the condensed and free atomic systems, respectively, and $\phi(r_{ij})$ is a repulsive pair potential. The function $f(x)=1/[1+\exp(x)]$ is the Fermi function, and $\sigma(x)=-\{f(x)\ln(f(x))+[1-f(x)]\ln[1-f(x)]\}$ is the entropy density. The bond energy is the attractive contribution that leads to cohesion. The promotion energy is a repulsive energy due to the excitation of electrons from their free atomic ground state as atoms are brought together. The entropic term is the contribution to the free energy from the entropy due to the thermal excitation of electrons into empty states. The repulsive energy is the term that accounts for the repulsion of the ionic cores at short range. It has contributions from electrostatics, and from the repulsion of overlapping orbitals due to Pauli's principle.

The density matrix and Green's functions

Both the bond-order potential and the cluster method can be implemented by means of Green's functions, and both make use of the density matrix, so these are now described. The Lanczos algorithm and auxiliary space are useful mathematical tools for developing the formalism (and for numerical implementation) so are also described here.

The band energy and forces can be written in terms of the *density matrix* $\rho_{i\alpha,j\beta}$ (the off-diagonal components of which are also called bond orders):

$$\begin{aligned}E_{coh}&=2\sum_{i\alpha,j\beta}H_{i\alpha,j\beta}\rho_{j\beta,i\alpha}-\sum_{i\alpha}\varepsilon_{i\alpha}N^0_{i\alpha}+\frac{1}{2}\sum_{i\neq j}\phi(r_{ij})\\&\quad-2k_BT\sum_{i\alpha}\int\sigma[(E-\mu)/k_BT]n_{i\alpha}(E)dE,\\F_\lambda&=-2\sum_{i\alpha,j\beta}\frac{\partial H_{i\alpha,j\beta}}{\partial\lambda}\rho_{j\beta,i\alpha}-\frac{1}{2}\sum_{i\neq j}\frac{\partial\phi(r_{ij})}{\partial\lambda}.\end{aligned}\tag{2}$$

Here λ is an atomic coordinate, and $F_\lambda=-\partial E_{coh}/\partial\lambda$.

The operator expression for the single-particle Green's function $(\hat{G}(Z))$ is $(Z-\hat{H})\hat{G}(Z)=\hat{1}$. Matrix elements of the Green's function can be taken, to which we give the following notation: $G_{i\alpha,j\beta}(Z)=\langle i\alpha|\hat{G}(Z)|j\beta\rangle$. The matrix equation for the Green's function is then

$$\sum_{k\gamma}(Z\delta_{i,k}\delta_{\alpha,\gamma}-H_{i\alpha,k\gamma})G_{k\gamma,j\beta}(Z)=\delta_{i,j}\delta_{\alpha,\beta}.\tag{3}$$

The density matrix is obtained from the Green's function through the following equation:

$$\rho_{i\alpha,j\beta}=-\frac{1}{\pi}\,\mathrm{Im}\left\{\int dE G_{i\alpha,j\beta}(E+\mathrm{i}0^+)f[(E-\mu)/k_BT]\right\},\tag{4}$$

where 0^+ stands for a positive infinitesimal. A robust scheme for carrying out integrals over energy of the product of the Fermi function and a function of energy that is analytic off the real axis is given in Appendix A.

A very stable, and rapidly convergent, method for calculating the diagonal elements of the Green's-function matrix is the recursion method.[22] This is based on the Lanczos algorithm,[28] which is an efficient way of tridiagonalizing a matrix. The central equation is

$$\hat{H}|U_n\rangle=a_n|U_n\rangle+b_n|U_{n-1}\rangle+b_{n+1}|U_{n+1}\rangle.\tag{5}$$

The states $|U_n\rangle$ are orthonormal ($\langle U_n|U_m\rangle=\delta_{n,m}$), and tridiagonalize the Hamiltonian:

$$\langle U_m|\hat{H}|U_n\rangle=\begin{cases}a_n & \text{if } m=n,\\ b_n & \text{if } m=n-1,\\ b_{n+1} & \text{if } m=n+1,\\ 0 & \text{otherwise.}\end{cases}\tag{6}$$

The matrix element of the Green's function $G_{00}(Z)=\langle U_0|\hat{G}(Z)|U_0\rangle$ is obtained from the recursion coefficients a_n and b_n as a continued fraction:

$$G_{00}(Z)=\cfrac{1}{Z-a_0-\cfrac{b_1^2}{Z-a_1-\cfrac{b_2^2}{Z-a_2-\cfrac{b_3^2}{\ddots}}}}.\tag{7}$$

To obtain the diagonal Green's-function matrix element $G_{i\alpha,i\alpha}(Z)$ then, it is merely necessary to begin the recursion process with $|U_0\rangle=|i\alpha\rangle$, and then use Eqs. (6) and (7). For an infinite system, there could be an infinite number of levels in the continued fraction. It is often the case, however, that the exact values can be replaced by estimated values after a certain number of levels, without reducing the accuracy significantly. The simplest approximation is to take $a_n=a_\infty, b_n=b_\infty$ for $n>N$, where N is the number of exact levels, and a_∞ and b_∞ are constants defining the band center and bandwidth.[29] The constant terms can be summed exactly to form the square root terminator:

$$t(Z)=\cfrac{1}{Z-a_\infty-\cfrac{b_\infty^2}{Z-a_\infty-\cfrac{b_\infty^2}{Z-a_\infty-\cfrac{b_\infty^2}{\ddots}}}}$$

$$=\frac{1}{b_\infty}\left[\left(\frac{Z-a_\infty}{2b_\infty}\right)-i\sqrt{1-\left(\frac{Z-a_\infty}{2b_\infty}\right)^2}\right]. \tag{8}$$

The other matrix elements $[G_{nm}(Z)=\langle U_n|\hat{G}(Z)|U_m\rangle]$ are obtained from another recurrence relationship which follows directly from the definition of the Green's function and the states $|U_n\rangle$:

$$(Z-a_n)G_{nm}(Z)-b_nG_{n-1,m}(Z)-b_{n+1}G_{n+1,m}(Z)=\delta_{n,m}. \tag{9}$$

Both of the methods to be described below can be formulated most easily if an auxiliary space is first introduced. Let vectors in this space be represented by the following symbols: $|e_\nu)$. The inner product between two vectors will be given the symbol

$$\Lambda_{\nu,\nu'}=(e_\nu|e_{\nu'}). \tag{10}$$

Operators that operate on the Hilbert space, auxiliary space, and both spaces will be indicated by a hat (e.g., $\hat{H}$ for the Hamiltonian), a bar (e.g., $\bar{a}_n$ for a cluster recursion coefficient), and a tilde (e.g., $\tilde{P}_n$ for a cluster recursion state), respectively.

III. MOMENTS-BASED METHODS

A convenient way to describe the density of states is in terms of its *moments*, where the pth moment ($\mu_{i\alpha}^p$) of the projected density of states $n_{i\alpha}(E)$ is given by $\mu_{i\alpha}^p=\int E^p n_{i\alpha}(E)dE$. The first moment ($\mu_{i\alpha}^1$) defines the middle of the band, the second moment ($\mu_{i\alpha}^2$) its width, the third moment ($\mu_{i\alpha}^3$) gives a measure of how skewed the band is, the fourth moment ($\mu_{i\alpha}^4$) determines whether the density of states is unimodal or bimodal, and so on. For a smooth density of states, using only the first few *exact* moments it is possible to make a good estimate of its shape. In fact the first and second moments alone (which do not even define a shape, but only a band center and width) can give a good approximation for the band energies.[30]

There is a useful identity[21] which is that the pth moment of the density of states projected onto orbital $|\psi\rangle$ ($n_\psi(E)$) equals the pth moment of the Hamiltonian projected onto the same orbital:

$$\mu_\psi^p=\int E^p n_\psi(E)dE=\langle\psi|\hat{H}^p|\psi\rangle. \tag{11}$$

This allows us to evaluate the moments of the projected density of states from the Hamiltonian matrix. Substituting the Hamiltonian matrix for the operator in Eq. (11), and putting $|\psi\rangle=|i\alpha\rangle$, we obtain

$$\mu_{i\alpha}^p=\sum_{j_1\beta_1\ldots j_{p-1}\beta_{p-1}} H_{i\alpha,j_1\beta_1}H_{j_1\beta_1,j_2\beta_2}\ldots H_{j_{p-1}\beta_{p-1},j\beta}. \tag{12}$$

This equation reveals a correspondence between the pth moment and a process of hopping around the lattice along closed paths of length p. Thus the first moment corresponds to a hop on a single site, the second to hops to nearest neighbors and back, and so on. Therefore, increasing the order of the moments by *two* corresponds to obtaining information about *one* extra shell of atoms since you have to hop out and back. This direct correspondence between electronic structure and the positions of atoms can give immediate insight into the nature of cohesion provided not too many moments are needed for an adequate description of the density of states.

A. The bond-order potential

By direct evaluation of the first few recursion coefficients using Eq. (5), with the condition that $|u_0\rangle=|i\alpha\rangle$, it is straightforward to show that

$$\mu_{i\alpha}^0=1,\quad \mu_{i\alpha}^1=a_0,\quad \mu_{i\alpha}^2=a_0^2+b_1^2,$$

$$\mu_{i\alpha}^3=a_0^3+2a_0b_1^2+a_1b_1^2,$$

$$\mu_{i\alpha}^4=a_0^4+3a_0^2b_1^2+2a_0a_1b_1^2+a_1^2b_1^2+b_1^2b_2^2+b_1^4. \tag{13}$$

Thus increasing the number of recursion levels corresponds directly to increasing the number of moments. The recursion method can then be understood as an optimal way of obtaining the density of states from moments of the Hamiltonian, and as such allows for a straightforward interpretation of cohesion in terms of *local* arrangements of atoms.

Although the diagonal elements of the Green's-function matrix are sufficient for the evaluation of cohesive energy [see Eq. (1)], off-diagonal elements are needed for the evaluation of forces [see Eqs. (2) and (4)]. The bond-order potential is a way of extending the above ideas to allow the evaluation of the off-diagonal elements of the Green's-function matrix which retains the moment description of bonding.

The first step is to create a new set of state vectors that belong to the product space formed from the Hilbert and auxiliary spaces. In particular consider the state

$$|W_0^\Lambda\}=\sum_{i\alpha}|e_{i\alpha})|i\alpha\rangle. \tag{14}$$

The expectation value of the Green's-function operator with respect to this state is then

$$G_{00}^\Lambda(Z)=\frac{\{W_0^\Lambda|\hat{G}(Z)|W_0^\Lambda\}}{\{W_0^\Lambda|W_0^\Lambda\}}$$

$$=\frac{\Sigma_{i\alpha,j\beta}\langle i\alpha|(e_{i\alpha}|\hat{G}(Z)|e_{j\beta})|j\beta\rangle}{\Sigma_{i\alpha,j\beta}\langle i\alpha|(e_{i\alpha}|e_{j\beta})|j\beta\rangle}$$

$$=\frac{\Sigma_{i\alpha,j\beta}\langle i\alpha|\hat{G}(Z)|j\beta\rangle(e_{i\alpha}|e_{j\beta})}{\Sigma_{i\alpha,j\beta}\langle i\alpha|j\beta\rangle(e_{i\alpha}|e_{j\beta})}$$

$$=\frac{\Sigma_{i\alpha,j\beta}G_{i\alpha,j\beta}(Z)\Lambda_{i\alpha,j\beta}}{\Sigma_{i\alpha}\Lambda_{i\alpha,i\alpha}}, \tag{15}$$

and hence

$$G_{i\alpha,j\beta}(Z)=\frac{\partial G^{\Lambda}_{00}(Z)}{\partial \Lambda_{i\alpha,j\beta}}+G^{\Lambda}_{00}(Z)\,\delta_{i,j}\delta_{\alpha,\beta}, \tag{16}$$

where we have now taken $\Sigma_{i\alpha}\Lambda_{i\alpha,i\alpha}=1$. The Green's function $G^{\Lambda}_{00}(Z)$ is evaluated using Eq. (7), but the recursion coefficients are obtained from the following modified version of Eq. (5):

$$\hat{H}|W^{\Lambda}_n\}=a^{\Lambda}_n|W^{\Lambda}_n\}+b^{\Lambda}_n|W^{\Lambda}_{n-1}\}+b^{\Lambda}_{n+1}|W^{\Lambda}_{n+1}\}, \tag{17}$$

with the condition

$$\{W^{\Lambda}_n|W^{\Lambda}_m\}=\delta_{m,n}. \tag{18}$$

Thus we have the following expression for the *off-diagonal* elements of the Green's function:

$$\begin{aligned}G_{i\alpha,j\beta}(Z)&=\sum_{n=0}^{\infty}\frac{\partial G^{\Lambda}_{00}(Z)}{\partial a^{\Lambda}_n}\frac{\partial a^{\Lambda}_n}{\partial \Lambda_{i\alpha,j\beta}}+\sum_{n=1}^{\infty}\frac{\partial G^{\Lambda}_{00}(Z)}{\partial b^{\Lambda}_n}\frac{\partial b^{\Lambda}_n}{\partial \Lambda_{i\alpha,j\beta}}\\&=\sum_{n=0}^{\infty}G^{\Lambda}_{0n}(Z)G^{\Lambda}_{n0}(Z)\frac{\partial a^{\Lambda}_n}{\partial \Lambda_{i\alpha,j\beta}}\\&\quad+2\sum_{n=1}^{\infty}G^{\Lambda}_{0(n-1)}(Z)G^{\Lambda}_{n0}(Z)\frac{\partial b^{\Lambda}_n}{\partial \Lambda_{i\alpha,j\beta}}.\end{aligned} \tag{19}$$

Combining Eqs. (4) and (19) we obtain

$$\rho_{i\alpha,j\beta}=-\left[\sum_{n=0}^{\infty}\chi^{\Lambda}_{0n,n0}\frac{\partial a^{\Lambda}_n}{\partial \Lambda_{i\alpha,j\beta}}+2\sum_{n=1}^{\infty}\chi^{\Lambda}_{0(n-1),n0}\frac{\partial b^{\Lambda}_n}{\partial \Lambda_{i\alpha,j\beta}}\right], \tag{20}$$

where

$$\chi^{\Lambda}_{0m,n0}=\frac{1}{\pi}\,\mathrm{Im}\left\{\int dE\,G^{\Lambda}_{0m}(E+\mathrm{i}0^{+})G^{\Lambda}_{n0}(E+\mathrm{i}0^{+})\times f[(E-\mu)/k_BT]\right\}. \tag{21}$$

The details of how the derivatives of the recursion coefficients are evaluated can be found in Appendix B.

In many TB simulations, local charge neutrality (LCN) is imposed as the simplest form of self-consistency.[3] Within the BOP scheme, this can be applied very efficiently since we know the response functions. If the excess charge on site i is Q_i, then a good estimate of the shift that should be applied to the on-site energies is

$$\Delta_i=-Q_i/X_i, \tag{22}$$

where $X_i=-2\Sigma_{\alpha}\chi^{\Lambda}_{00,00}$, since $-2\chi^{\Lambda}_{00,00}=\partial N^{\Lambda}/\partial a^{\Lambda}_0$, and $a^{\Lambda}_0=\varepsilon_{i\alpha}$. Using this prescription, usually no more than three or four iterations are needed to achieve convergence.

As a first test of the quality of the BOP forces, we performed a constant energy molecular-dynamics simulation of silicon in the diamond structure at 500 K using a time step of 1.0 fs. Five recursion levels were used with the square root terminator. In Fig. 1 is shown the energy as a function of time. It is clearly well conserved, indicating that the forces are of good quality.

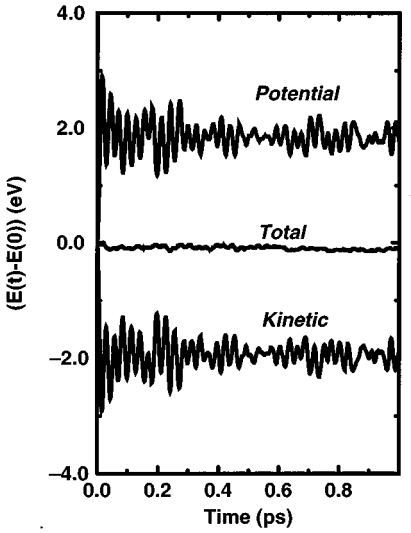

FIG. 1. The potential, kinetic, and total energy as a function of time for a molecular-dynamics simulation of silicon in the diamond structure. The time step is 1.0 fs.

B. The scaling of CPU time with number of moments

The calculation of moments is most efficiently done with the use of Eq. (12) rewritten as $\mu^{p}_{i\alpha}=\langle u^{p_1}|u^{p_2}\rangle$, where $u^{r}=H^{r}|i\alpha\rangle$, $p_1=[p/2]$, and $p_2=p-p_1$. It is easy to estimate number of operations needed to calculate the vectors $|u^{r}\rangle$. Each multiplication by H propagates the wave function from the origin and involves $\propto i^3$ sites after i hops to nearest neighbors. At the next step, to evaluate $H|u^{i}\rangle$ we have to perform $\sim \nu i^3$ multiplications, where ν is equal to the number of nearest neighbors, z, times the number of orbitals per atom, n_o. The total number of operations to get the first p moments is thus given approximately by $N_{op}\sim\Sigma_i^{p/2} z n_o i^3 \sim z n_o (p/2)^4$. This expression definitely *overestimates* the required number of operations. This is because many paths contributing to μ_p wind about the origin, making the effective size of cluster grow $\propto i^{3/2}$, as in the case of a random walk. In this case the required number of iterations would be $\sim z(p/2)^{5/2}$. As a result, the true number of operations must lie in the interval $z n_o (p/2)^{5/2} < N_{op} < z n_o (p/2)^4$.

We have performed the calculations for Si ($z=4$) and Ti ($z=12$) and found that the cluster size and the CPU time grow marginally faster than the third power of the number of moments (Fig. 2). These calculations confirm also that the number of operations grows linearly with number of neighbors.

IV. CLUSTER RECURSION

The moments-based methods are usually expected to achieve convergence only with the use of many moments for some strongly covalent systems where high resolution of the peaks in the density of states is required. Based on the observation much used in chemistry that bonds can be treated in a completely local manner, one would expect convergence to improve considerably by partitioning the system into small clusters containing the first-neighbor shell of atoms, solving the clusters exactly and then *recurring on the clus-*

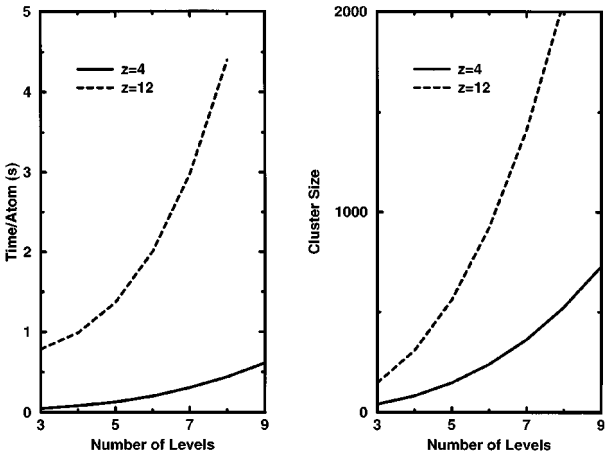

FIG. 2. CPU time in seconds and exact cluster size needed for a single evaluation of force in Si (coordination number $z=4$, number of orbitals per site $n_o=4$) and Ti ($z=12$ and $n_o=5$) versus the number of recursion levels. The calculations were carried out on HP Apollo 9000/735 workstations.

ters. If longer-ranged effects are less important, the rest of the system can be viewed as a perturbation on this. This is achieved by cluster recursion (CR),[31] which is very similar to matrix recursion.[32–34]

First we reexpress the central results in terms of an auxiliary space to show the similarities and differences between this formalism, and that of BOP, then we describe some characteristics of the method, and finally give some details concerning its implementation.

Consider the projection operators

$$\tilde{P}_n=\sum_{i\alpha}\ |n;i\alpha\rangle(e_{i\alpha}| \tag{23}$$

that operate both in the Hilbert and auxiliary spaces, where $|0;i\alpha\rangle=|i\alpha\rangle$. They satisfy the following recursion relation:

$$\hat{H}\tilde{P}_n=\tilde{P}_n\bar{a}_n+\tilde{P}_{n-1}\bar{b}_n+\tilde{P}_{n+1}\bar{b}_{n+1}. \tag{24}$$

Provided the auxiliary space vectors are orthonormal, we have the following identities:

$$\bar{I}=\sum_{i\alpha}\ |e_{i\alpha})(e_{i\alpha}|, \quad \tilde{P}_n^{\dagger}\tilde{P}_m=\delta_{nm}\bar{I},$$

$$\bar{a}_n=\tilde{P}_n^{\dagger}\hat{H}\tilde{P}_n, \quad \bar{b}_n=\tilde{P}_{n-1}^{\dagger}\hat{H}\tilde{P}_n. \tag{25}$$

The Green's function $\bar{G}_{00}(Z)$ is given by [compare with Eq. (7)]

$$\bar{G}_{00}(Z)=[Z\bar{I}-\bar{a}_0-\bar{b}_1^{\dagger}[Z\bar{I}-\bar{a}_1-\bar{b}_2^{\dagger}[\ \dots\ ]^{-1}\bar{b}_2]^{-1}\bar{b}_1]^{-1}. \tag{26}$$

From this we get

$$G_{i\alpha,j\beta}(Z)=(i\alpha|\bar{G}_{00}(Z)|j\beta). \tag{27}$$

The CR method works with a cluster, which is defined by the list of orbitals $|i\alpha\rangle$ appearing in the sum in Eq. (23). In this work we take the first-neighbor shell of atoms about a site. This results in the following: all the elements of the Green's function (and hence the density matrix) needed to evaluate the energy and forces on the central atom are calculated simultaneously; the first-neighbor shell cluster is treated exactly in the absence of any other atoms (subsequent shells act as a perturbing medium); the two expressions for the bond energy [Eqs. (1) and (2)] are guaranteed to give identical answers. The first point follows from Eq. (27), the second from Eq. (26) with b_1 set to zero (the Green's function is then exact for the cluster, since $\bar{a}_0$ is the Hamiltonian for the cluster), and the third from the fact that the same Green's function is used both for the local density of states and the density matrix.

As with BOP, we take only a finite number of exact levels, and then estimate the remaining levels. In this work we use a square root terminator, formulated in the following way. Consider the innermost level in Eq. (26). We write this as $[Z\bar{I}-\bar{a}_N-\bar{b}_{\infty}^{\dagger}\bar{T}(Z)\bar{b}_{\infty}]$. Here $T(Z)$ is the terminator. To obtain a closed form for the terminator that retains the symmetry properties of the Green's function, we set [compare with Eq. (8)]

$$\bar{T}(Z)=[Z\bar{I}-\bar{a}_N-\bar{b}_{\infty}^{\dagger}\bar{T}(Z)\bar{b}_{\infty}]^{-1}. \tag{28}$$

This is still a difficult set of equations to solve, so to simplify matters we assume that $\bar{b}_{\infty}$ and $\bar{T}(Z)$ commute with $\bar{a}_N$. Thus, if we diagonalize $\bar{a}_N$, to give $\bar{a}_N=\Sigma_{\lambda}|\lambda)\epsilon_{\lambda}(\lambda|$, we can also write $b_{\infty}=\Sigma_{\lambda}|\lambda)b_{\lambda}(\lambda|$ and $T(Z)=\Sigma_{\lambda}|\lambda)t_{\lambda}(Z)(\lambda|$. Hence we can reexpress Eq. (28) as

$$\begin{aligned} t_{\lambda}(Z)&=[Z-\epsilon_{\lambda}-b_{\lambda}t_{\lambda}(Z)b_{\lambda}]^{-1} \\ &=\frac{1}{b_{\lambda}}\left[\left(\frac{Z-\epsilon_{\lambda}}{2b_{\lambda}}\right)-i\sqrt{1-\left(\frac{Z-\epsilon_{\lambda}}{2b_{\lambda}}\right)^2}\right]. \end{aligned} \tag{29}$$

Thus we see that the effect of the terminator is to smear out the sharp states with energies ϵ_{λ} into semielliptical bands. The degree of smearing is given by b_{λ}. These are taken to be of all the same value, given by the average of the diagonal elements of $\bar{b}_N$.

Again, LCN can be imposed very efficiently by means of Eq. (22), where now $X_i=-(2/\pi)\mathrm{Im}\{\Sigma_{\alpha}\int dE[G_{i\alpha,i\alpha}(E+i0^+)]^2 f[(E-\mu)/k_BT]\}$.

V. COMPARISON OF CONVERGENCE PROPERTIES

We are now in a position to compare the two methods, and so acquire some insight into the properties of moments methods. We have performed a series of comparisons, looking at the convergence of energy and forces as a function of number of recursion levels, and also the time to calculate the energy and forces once for one atom. These comparisons have been carried out on a metal (titanium), a semiconductor (silicon), and a covalent molecule (benzene).

First we consider rate of convergence *with respect to number of levels*. From Fig. 3, we note that for titanium the bulk cohesive energy converges at about the same rate for the two methods, which follows from the fact that the density of states is smooth. However, the force on an atom at the (100) surface converges more rapidly and more smoothly with CR than with BOP. From Fig. 4, we see that CR gives slightly better energy convergence than BOP for bulk silicon, somewhat better convergence for the vacancy formation energy, and much better convergence for the force on an atom

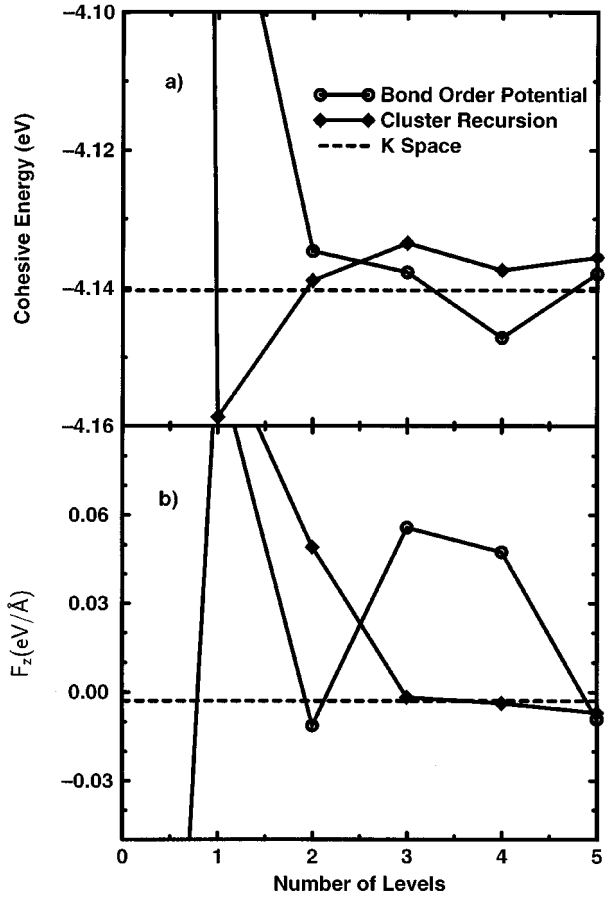

FIG. 3. The cohesive energy for bulk titanium (a) and the force on an atom at the unrelaxed (100) surface (b) as a function of number of recursion levels for the bond-order potential and cluster recursion.

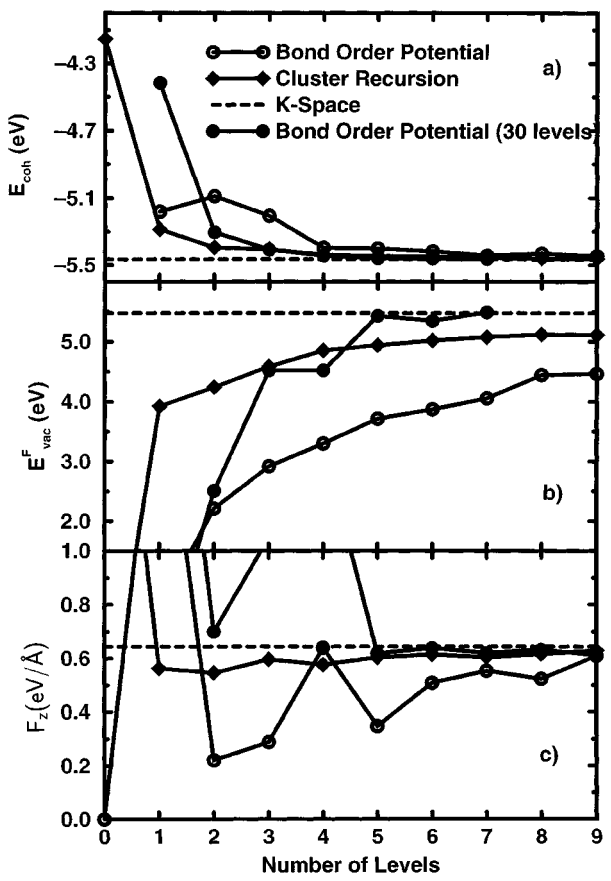

FIG. 4. The cohesive energy for bulk silicon (a), the unrelaxed vacancy formation energy (b), and the force on an atom at the unrelaxed (100) surface (c) as a function of number of recursion levels for the bond-order potential and cluster recursion. The curves with filled circles are for BOP with 30 levels, but with the cluster size (defined as the number of exact levels that can be calculated within the cluster) varied.

at the (100) surface. It is clear that neither CR nor BOP are converging very rapidly to the correct vacancy formation energy at a moderate number of moments. This is because there are midgap states that are best modeled using a *k*-space approach. From Fig. 5, we see that for benzene, both the cohesive energy and the force on a hydrogen atom converge immediately with CR, but rather slowly with BOP.

There are two general observations that can be drawn from the above: for systems with smooth densities of states both methods give comparable rates of convergence with respect to number of levels for the energy, but for systems with structured densities of states corresponding to localized bonding, CR gives better convergence for the same number of moments; CR gives better force convergence.

From these observations we can conclude that forces are dominated by the short-range contributions to cohesion, and that the errors observed in calculations for covalent systems made with moments-based methods follow from the incomplete description of the local atomic environment. The way around this problem is to take many levels on a cluster of small size. The major criticism of this approach is that the clusters have free surfaces, so that the density of states may acquire spurious peaks due to surface states.

Despite this objection, we have tried this approach from within the BOP formalism (but without any terminator). We used 30 levels, and varied the cluster size. The size of the cluster is determined by the number of hops it takes to reach the outside from the center (this is equal to the number of exact levels that can be obtained from the cluster). We are thus interested in the rate of convergence *with respect to cluster size*. From Fig. 5 it is clear that convergence is achieved with a very small cluster (two levels) for benzene, as expected given the rapid convergence of CR. From Fig. 4 it is clear that the cohesive energy, force, and vacancy formation energy for silicon converge rapidly using this approach. The insensitivity of the results to cluster size beyond a critical size follows from the finite range of the density matrix.

Having established the physical principles governing convergence for covalent systems, we now address the practicalities of computer simulations. What matters in this case is the rate of convergence *with respect to computer time*. The timings for the test calculations described above were all carried out on HP Apollo 9000/735 workstations. When working with *exact* levels, we see from Figs. 6, 7, and 8 that the time scales with number of levels in the same way for the two methods, but that CR is slower than BOP by a constant factor for a given system and number of levels. This factor is proportional to the cube of the number of orbitals in the CR cluster, thus it becomes *very* slow for close packed systems

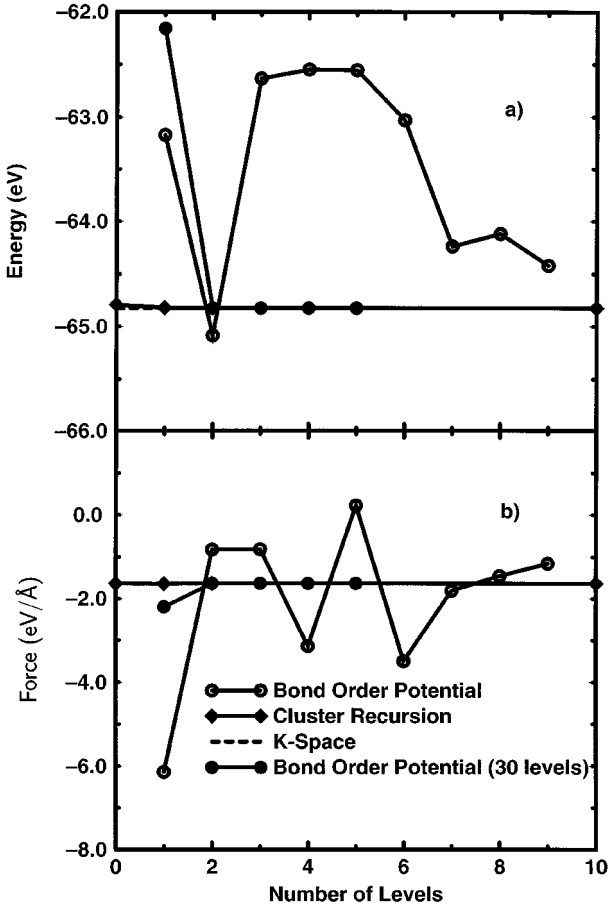

FIG. 5. The cohesive energy for a benzene molecule (a), and the force on a hydrogen atom (b) as a function of number of recursion levels for the bond-order potential and cluster recursion. The curves with filled circles are for BOP with 30 levels, but with the cluster size (defined as the number of exact levels that can be calculated within the cluster) varied.

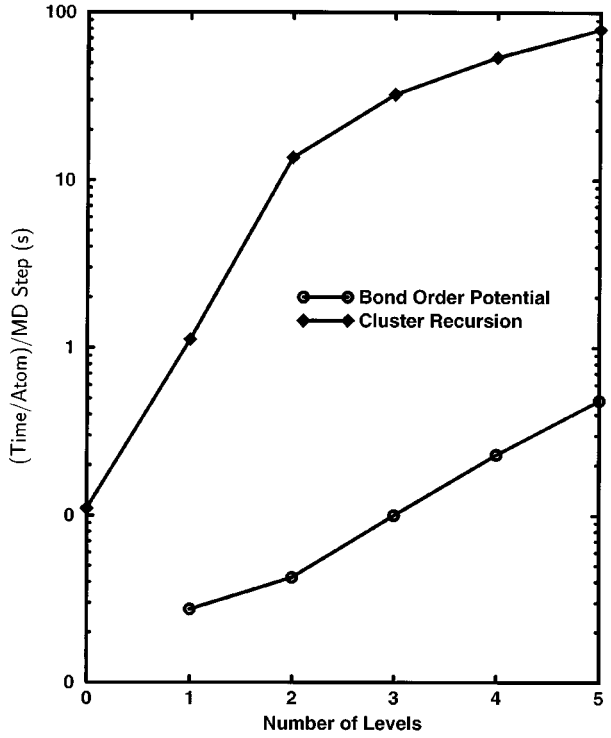

FIG. 6. The time to carry out the energy and force evaluation for one atom as a function of number of levels for the bond-order potential and the cluster recursion in bulk titanium. The calculations were carried out on HP Apollo 9000/735 workstations. Note the logarithmic time scale.

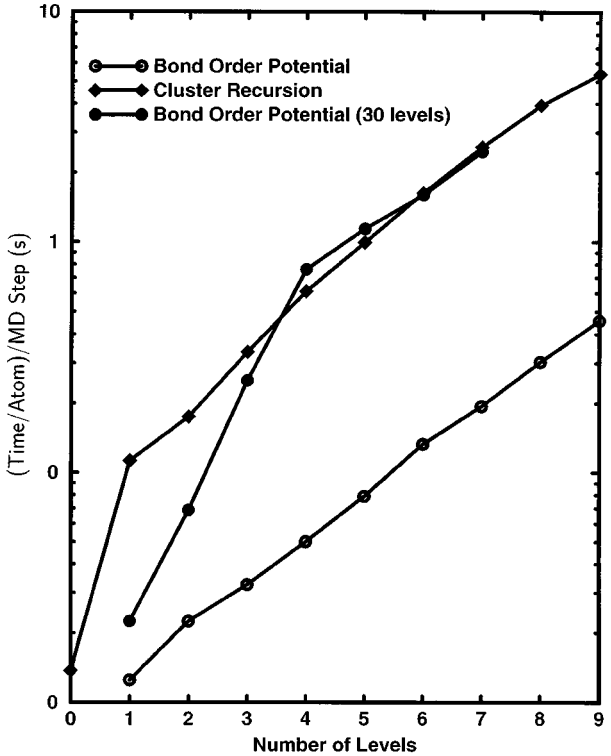

FIG. 7. The time to carry out the energy and force evaluation for one atom as a function of number of levels for the bond-order potential and the cluster recursion in bulk silicon. The calculations were carried out on HP Apollo 9000/735 workstations. Note the logarithmic time scale. The curve with filled circles is for BOP with 30 levels, but with the cluster size (defined as the number of exact levels that can be calculated within the cluster) varied.

with large numbers of orbitals per atom, though rather less so for low-coordination structures with few orbitals per atom. For covalent systems we have established that BOP should be used with many levels taken within a small cluster. In this case we see from Fig. 8 that BOP is about a factor of 3 times faster than CR for benzene. From Fig. 7, we find that for silicon the two methods are comparable in speed for the cluster sizes needed for stable forces. However, it may be the case that fewer than 30 levels can be used, in which case BOP will be faster than CR. The general conclusion then is that BOP converges faster with respect to CPU time than CR.

CR could be used with a fixed cluster size within which many levels are taken. This would create two time savings: the recursion is performed for smaller clusters, thus is faster to perform; the integrals can be performed exactly by diagonalizing the block tridiagonal Hamiltonian thus avoiding the need to perform multiple inversions of complex matrices. This has been investigated briefly, and it was discovered that, for extended systems, the benefits of the terminator outweighed the benefits of diagonalizing the block-diagonal Hamiltonian. While it is still possible to use a fixed cluster with a terminator, and thus introduce some time savings, these will be small as most time is spent inverting matrices that are independent of cluster size, until very large clusters

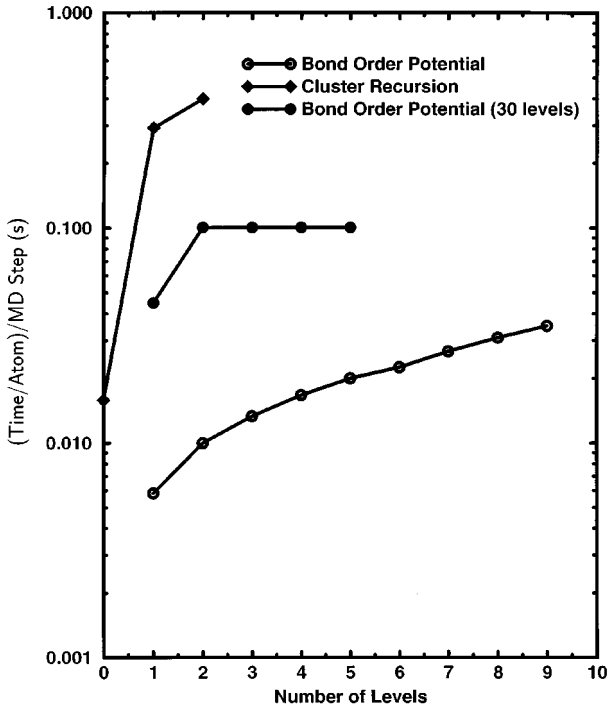

FIG. 8. The time to carry out the energy and force evaluation for one atom as a function of number of levels for the bond-order potential and the cluster recursion in benzene. The calculations were carried out on HP Apollo 9000/735 workstations. Note the logarithmic time scale. The curve with filled circles is for BOP with 30 levels, but with the cluster size (defined as the number of exact levels that can be calculated within the cluster) varied.

are formed. Thus the fixed cluster approach is only likely to be useful for molecules.

It is useful to compare the timings of the above methods with the corresponding times for direct diagonalization of the Hamiltonian. This tells us when it is more efficient to use an $O(N)$ method. In Fig. 9 is shown the time to evaluate the energy and forces for a cell containing silicon in the diamond structure as a function of the number of atoms in the cell, for

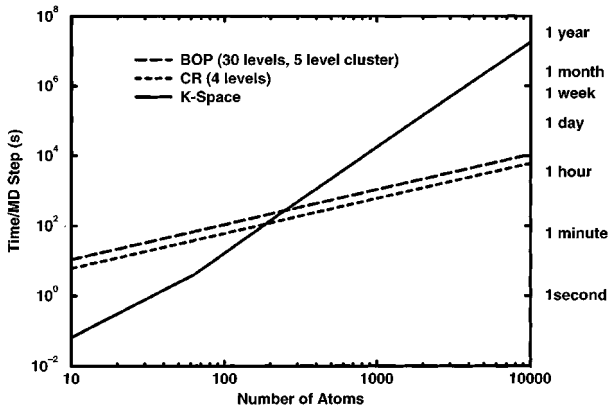

FIG. 9. The time to carry out the energy and force evaluation for silicon as a function of number of atoms in the computational cell for the bond-order potential, cluster recursion, and K space. The calculations were carried out on HP Apollo 9000/735 workstations. Note the logarithmic time scale. The crossover point at which the $O(N)$ methods become favorable is about 200 atoms.

BOP, CR, and k space, using a single k point. Diagonalization is most efficient up to about 200 atoms, after which the $O(N)$ methods become more efficient.

VI. CONCLUSIONS

For an atomistic modeling method to be useful it must provide good estimates of cohesive energies and atomic forces with a minimum of computational effort, and in such a way as to allow straightforward interpretation of results. The TB model of cohesion is presented as a successful theory for describing cohesion in a wide range of materials which often allows considerable insight into bonding to be obtained.

The problem of evaluating atomic forces and cohesive energy in large systems using TB is discussed, and two methods (BOP and CR) which overcome this problem are presented. BOP is taken as a particularly appropriate moments-based method for atomistic simulations, whereas CR is considered as it treats first-neighbor contributions to bonds exactly.

Both methods allow straightforward interpretations of bonding in terms of local atomic structure, provided they converge at a few levels. Furthermore, they both provide linear scaling of computer time with system size, and are naturally parallel methods.

Convergence with respect to three different quantities is considered: number of levels, cluster size at fixed large number of levels, and CPU time. For convergence *with respect to number of levels* it is found that: for titanium (a metal), both cohesive energy and atomic forces converge rapidly for BOP or CR; for silicon (a semiconductor) the bulk cohesive energy converges rapidly for both BOP and CR, though CR gives much more rapid force convergence, and both give poor convergence for the isolated vacancy formation energy; for benzene (a molecule) BOP gives slow energy and force convergence whereas CR gives rapid force convergence. From these observations we can conclude that forces are dominated by the short-range contributions to cohesion, and that the errors observed in calculations for covalent systems made with moments-based methods follow from the incomplete description of the local atomic environment. The way around this problem is to take many levels on a cluster of small size. If BOP is now used with many levels (30 in this work), but the cluster in which the levels are taken is allowed to vary, it is found that BOP gives rapid convergence *with respect to cluster size* for energies and forces for benzene and silicon, *even for the vacancy formation energy*. BOP gives better convergence *with respect to CPU time* than CR in all cases.

ACKNOWLEDGMENTS

The authors would like to thank M. Fearn and A.P. Sutton for many useful discussions. This work was carried out using the computational facilities of the Materials Modelling Laboratory (MML) in the Department of Materials at Oxford University. The MML was partially funded by SERC Grant No. GR/H58278. A.H. and M.A. would like to thank Hewlett-Packard and NEDO (Japan), respectively, for their financial support.

APPENDIX A

The calculation of energies and response functions at finite electron temperature requires integrations with the Fermi function. This is customarily carried out in the complex plane by summing up an infinite series over the Matsubara poles.[35] The convergence of this series is, however, *very* slow. A much more efficient scheme is now described.

It is possible to accelerate considerably the Matsubara summation by using the following approximant for the exponential function:

$$\exp(Z)\approx\left(1+\frac{Z}{n}\right)^n \tag{A1}$$

which becomes *exact* as n tends to infinity. This gives the following very useful representation for the Fermi function:

$$f(E)=\frac{1}{\exp(\beta(E-\mu))+1}\approx\frac{1}{\left(1+\dfrac{\beta(E-\mu)}{2M}\right)^{2M}+1}, \tag{A2}$$

where $\beta=1/K_BT$, and μ is the chemical potential. This approximation (which becomes exact in the limit of large M) has $2M$ simple poles (E_p) located on a circle in the complex plane off the real axis

$$E_p=\mu+\frac{2M}{\beta}(z_p-1),\quad z_p=\exp(i\pi(2p+1)/2M),$$

$$p=0,1,\ldots,2M-1 \tag{A3}$$

with residues $R_p=-z_p/\beta$.

Now we can write the equation for the bond energy of individual sites [see Eq. (1)] in the following simple form:

$$E_{bond}^{i\alpha}=\frac{4}{\beta}\,\mathrm{Re}\sum_{p=0}^{M-1} z_p(E_p-\epsilon_{i\alpha})G_{i\alpha,i\alpha}(E_p), \tag{A4}$$

where $G_{00}^{i\alpha}(Z)=\langle i\alpha|(Z-\hat{H})^{-1}|i\alpha\rangle$. Analogously, we obtain the following expressions for the response functions [see Eq. (21)] and the number of electrons:

$$\chi_{0m,n0}^{i\alpha}=-\frac{2}{\beta}\,\mathrm{Re}\sum_{p=0}^{M-1} z_pG_{0m}^{i\alpha}(E_p)G_{n0}^{i\alpha}(E_p)$$

$$N^{i\alpha}=\frac{4}{\beta}\,\mathrm{Re}\sum_{p=0}^{M-1} z_pG_{00}^{i\alpha}(E_p), \tag{A5}$$

with $G_{0m}^{i\alpha}(z)$ determined from Eq. (9). We find that typically 30 to 50 complex poles are enough to achieve convergence within about 12 digits. The calculation of $G_{00}^{i\alpha}$ is most efficiently performed by using the continuous fraction representation of Eq. (7) for the Green's function. The present method is found to be much more stable than analytical integration.[36] Moreover, the method is very general and may be used with any terminator, such as that which describes band gaps.[37]

APPENDIX B

Let us define the orthogonal polynomials $P_n^\Lambda(x)$:

$$xP_n^\Lambda(x)=b_n^\Lambda P_{n-1}^\Lambda(x)+a_n^\Lambda P_n^\Lambda(x)+b_{n+1}^\Lambda P_{n+1}^\Lambda(x), \tag{B1}$$

with $P_{-1}^\Lambda(x)=0$ and $P_0^\Lambda(x)=1$. The recursion vectors in the product space can be written as

$$|W_n^\Lambda\}=P_n^\Lambda(\hat{H})|W_0^\Lambda\}=\sum_{i\alpha} P_n^\Lambda(\hat{H})|i\alpha\rangle|e_{i\alpha}). \tag{B2}$$

Hence the recursion coefficients and orthonormality condition can be written as

$$\delta_{m,n}=\{W_m^\Lambda|W_n^\Lambda\}=\sum_{i\alpha,j\beta}\langle i\alpha|P_m^\Lambda(\hat{H})P_n^\Lambda(\hat{H})|j\beta\rangle\Lambda_{i\alpha,j\beta},$$

$$a_n^\Lambda=\{W_n^\Lambda|\hat{H}|W_n^\Lambda\}=\sum_{i\alpha,j\beta}\langle i\alpha|P_n^\Lambda(\hat{H})\hat{H}P_n^\Lambda(\hat{H})|j\beta\rangle\Lambda_{i\alpha,j\beta},$$

$$b_n^\Lambda=\{W_{n-1}^\Lambda|\hat{H}|W_n^\Lambda\}$$

$$=\sum_{i\alpha,j\beta}\langle i\alpha|P_{n-1}^\Lambda(\hat{H})\hat{H}P_n^\Lambda(\hat{H})|j\beta\rangle\Lambda_{i\alpha,j\beta}. \tag{B3}$$

If we now define the O matrix, which is given by

$$O_{i\alpha,j\beta}^{\Lambda,m,n}=\langle i\alpha|P_m^\Lambda(\hat{H})P_n^\Lambda(\hat{H})|j\beta\rangle, \tag{B4}$$

then we can write the derivatives of Eqs. (B3) as

$$0=O_{i\alpha,j\beta}^{\Lambda,m,n}+\left\{W_0^\Lambda\left|\frac{\partial P_m^\Lambda(\hat{H})}{\partial\Lambda_{i\alpha,j\beta}}P_n^\Lambda(\hat{H})\right|W_0^\Lambda\right\}$$

$$+\left\{W_0^\Lambda\left|P_m^\Lambda(\hat{H})\frac{\partial P_n^\Lambda(\hat{H})}{\partial\Lambda_{i\alpha,j\beta}}\right|W_0^\Lambda\right\},$$

$$\frac{\partial a_n^\Lambda}{\partial\Lambda_{i\alpha,j\beta}}=\langle i\alpha|P_n^\Lambda(\hat{H})\hat{H}P_n^\Lambda(\hat{H})|j\beta\rangle$$

$$+2\left\{W_0^\Lambda\left|\frac{\partial P_n^\Lambda(\hat{H})}{\partial\Lambda_{i\alpha,j\beta}}\hat{H}P_n^\Lambda(\hat{H})\right|W_0^\Lambda\right\},$$

$$\frac{\partial b_n^\Lambda}{\partial\Lambda_{i\alpha,j\beta}}=\langle i\alpha|P_{n-1}^\Lambda(\hat{H})\hat{H}P_n^\Lambda(\hat{H})|j\beta\rangle$$

$$+\left\{W_0^\Lambda\left|\frac{\partial P_{n-1}^\Lambda(\hat{H})}{\partial\Lambda_{i\alpha,j\beta}}\hat{H}P_n^\Lambda(\hat{H})\right|W_0^\Lambda\right\}$$

$$+\left\{W_0^\Lambda\left|P_{n-1}^\Lambda(\hat{H})\hat{H}\frac{\partial P_n^\Lambda(\hat{H})}{\partial\Lambda_{i\alpha,j\beta}}\right|W_0^\Lambda\right\}. \tag{B5}$$

Since $\partial P_n^\Lambda(x)/\partial\Lambda_{i\alpha,j\beta}$ is a polynomial of order less than or equal to m, it can be expressed as a linear combination of polynomials $P_r^\Lambda(x)$, with $r\leqslant m$. Consequently, the orthonormality condition given in (B3) implies

$$\left\{W_0^\Lambda\left|\frac{\partial P_m^\Lambda(\hat{H})}{\partial\Lambda_{i\alpha,j\beta}}P_n^\Lambda(\hat{H})\right|W_0^\Lambda\right\}=0\quad(\text{if } m<n). \tag{B6}$$

Using Eq. (B1) to eliminate $\hat{H}$ in Eq. (B5), and then substituting in Eqs. (B4) and (B6), we get

$$\frac{\partial a_n^\Lambda}{\partial \Lambda_{i\alpha,j\beta}} = b_{n+1}^\Lambda O_{i\alpha,j\beta}^{\Lambda,n+1,n} - b_n^\Lambda O_{i\alpha,j\beta}^{\Lambda,n,n-1},$$

$$2\frac{\partial b_n^\Lambda}{\partial \Lambda_{i\alpha,j\beta}} = b_n^\Lambda (O_{i\alpha,j\beta}^{\Lambda,n,n} - O_{i\alpha,j\beta}^{\Lambda,n-1,n-1}). \tag{B7}$$

From the following identity:

$$\langle i\alpha | P_{m-1}^\Lambda(\hat{H})(\hat{H} P_n^\Lambda(\hat{H})) | j\beta \rangle = \langle i\alpha | (P_{m-1}^\Lambda(\hat{H})\hat{H}) P_n^\Lambda(\hat{H}) | j\beta \rangle, \tag{B8}$$

we obtain the following recursive relation for the O matrix:

$$b_m^\Lambda O_{i\alpha,j\beta}^{\Lambda,m,n} + a_{m-1}^\Lambda O_{i\alpha,j\beta}^{\Lambda,m-1,n} + b_{m-1}^\Lambda O_{i\alpha,j\beta}^{\Lambda,m-2,n} = b_{n+1}^\Lambda O_{i\alpha,j\beta}^{\Lambda,m-1,n+1} + a_n^\Lambda O_{i\alpha,j\beta}^{\Lambda,m-1,n} + b_n^\Lambda O_{i\alpha,j\beta}^{\Lambda,m-1,n-1}. \tag{B9}$$

To apply this recursion relation, we need a set of starting matrices. The most natural choice is $O_{i\alpha,j\beta}^{\Lambda,n,0} = (e_{j\beta} | \langle i\alpha | W_n^\Lambda \rangle\}$. However, to generate $O_{i\alpha,j\beta}^{\Lambda,n,n}$, we need starting matrices up to $O_{i\alpha,j\beta}^{\Lambda,2n,0}$. This means that extra vectors $|W_n^\Lambda\rangle\}$ must be generated. This can be done using Eq. (17), but with arbitrary values of a_m^Λ and b_m^Λ for $m > n$, since the values of the derivatives of the recursion coefficients are independent of these values.

There are three sum rules that follow from Eq. (B7), and which are important. The first two ensure that the two expressions for the bond energy [Eqs. (1) and (2)] give the same results. The first sum rule is

$$\sum_{i\alpha,j\beta} \frac{\partial a_n^\Lambda}{\partial \Lambda_{i\alpha,j\beta}} \Lambda_{i\alpha,j\beta} = 0, \quad \sum_{i\alpha,j\beta} \frac{\partial b_n^\Lambda}{\partial \Lambda_{i\alpha,j\beta}} \Lambda_{i\alpha,j\beta} = 0. \tag{B10}$$

The second sum rule is

$$\sum_{i\alpha,j\beta,k\gamma} \frac{\partial a_n^\Lambda}{\partial \Lambda_{i\alpha,k\gamma}} \Lambda_{i\alpha,j\beta} H_{k\gamma,j\beta} = (b_{n+1}^\Lambda)^2 - (b_n^\Lambda)^2,$$

$$\sum_{i\alpha,j\beta,k\gamma} 2\frac{\partial b_n^\Lambda}{\partial \Lambda_{i\alpha,k\gamma}} \Lambda_{i\alpha,j\beta} H_{k\gamma,j\beta} = b_n^\Lambda [a_n^\Lambda - a_{n-1}^\Lambda]. \tag{B11}$$

The third sum rule relates the derivatives of the recursion coefficients to one another:

$$\sum_{n=0}^{N} \frac{\partial a_n^\Lambda}{\partial \Lambda_{i\alpha,j\beta}} = b_{N+1}^\Lambda O_{i\alpha,j\beta}^{\Lambda,N+1,N},$$

$$\sum_{n=1}^{N} \frac{2}{b_n^\Lambda} \frac{\partial b_n^\Lambda}{\partial \Lambda_{i\alpha,j\beta}} = O_{i\alpha,j\beta}^{\Lambda,N,N} - O_{i\alpha,j\beta}^{\Lambda,0,0}. \tag{B12}$$

These sum rules are used to truncate the expansion for the density matrix [Eq. (20)]. Only a finite number of exact recursion coefficients and their derivatives are ever calculated in practice. However, an infinite number of estimated recursion coefficients (the terminator) are added, and thus some way of introducing the corresponding estimated derivatives is needed (the truncator). We assume that a square root terminator is being used throughout. The right-hand sides of the first two sum rules [Eqs. (B10) and (B11)] are zero for $n \geq N+1$ for the derivatives of a_n^Λ, and for $n \geq N+2$ for the derivatives of b_n^Λ. Thus the simplest assumption is that the derivatives of the recursion coefficients are zero under these conditions, which makes the sums in Eq. (20) finite. Thus we need only find expressions for $\partial a_N^\Lambda / \partial \Lambda_{i\alpha,j\beta}$ and $\partial b_{N+1}^\Lambda / \partial \Lambda_{i\alpha,j\beta}$. If we assume that both $O_{i\alpha,j\beta}^{\Lambda,N+1,N}$ and $O_{i\alpha,j\beta}^{\Lambda,N+1,N+1}$ are linear in $\partial a_0^\Lambda / \partial \Lambda_{i\alpha,j\beta}$, then we obtain the following expressions by requiring that Eqs. (B10) and (B11) be satisfied:

$$\frac{\partial a_N^\Lambda}{\partial \Lambda_{i\alpha,j\beta}} = \left(\frac{b_\infty^\Lambda}{b_1^\Lambda}\right)^2 \frac{\partial a_0^\Lambda}{\partial \Lambda_{i\alpha,j\beta}} - b_N^\Lambda O_{i\alpha,j\beta}^{\Lambda,N,N-1},$$

$$2\frac{\partial b_{N+1}^\Lambda}{\partial \Lambda_{i\alpha,j\beta}} = b_\infty^\Lambda \delta_{i,j}\delta_{\alpha,\beta} + \frac{b_\infty^\Lambda (a_\infty^\Lambda - a_0^\Lambda)}{(b_1^\Lambda)^2} \frac{\partial a_0^\Lambda}{\partial \Lambda_{i\alpha,j\beta}} - b_\infty^\Lambda O_{i\alpha,j\beta}^{\Lambda,N,N}. \tag{B13}$$

*Present address: Department of Physics, Gifu University, 1-1 Yanagido, Gifu, 501-11, Japan.

[1] W. Kohn and L.J. Sham, Phys. Rev. **140**, A1133 (1965).
[2] J.C. Slater and G.F. Koster, Phys. Rev. **94**, 1498 (1954).
[3] A.P. Sutton, M.W. Finnis, D.G. Pettifor, and Y. Ohta, J. Phys. C **21**, 35 (1988).
[4] B. Legrand, Philos. Mag. B **49**, 171 (1984).
[5] B. Legrand, Philos. Mag. A **52**, 83 (1985).
[6] D.G. Pettifor, *Electron Theory in Alloy Design*, edited by D.G. Pettifor and A.H. Cottrell (Institute of Materials, London, 1992), p. 81.
[7] P.B. Allen, J.Q. Broughton, and A.K. McMahan, Phys. Rev. B **34**, 859 (1986).
[8] L. Goodwin, A.J. Skinner, and D.G. Pettifor, Europhys. Lett. **9**, 701 (1989).
[9] J.L. Mercer and M.Y. Chou, Phys. Rev. B **47**, 9366 (1993).
[10] D.J. Chadi, Phys. Rev. Lett. **43**, 43 (1979).
[11] F.S. Khan and J.Q. Broughton, Phys. Rev. B **39**, 3688 (1989).
[12] S. Sawada, *Ordering at Surfaces and Interfaces*, edited by A. Yoshimori *et al.* (Springer-Verlag, Berlin, 1986), p. 129.
[13] B.J. Min, Y.H. Lee, C.Z. Wang, C.T. Chan, and K.M. Ho, Phys. Rev. B **46**, 9677 (1992).
[14] C.Z. Wang, C.T. Chan, and K.M. Ho, Phys. Rev. Lett. **66**, 189 (1991).
[15] P.B. Allen and J.Q. Broughton, J. Phys. Chem. **91**, 4964 (1987).
[16] C.Z. Wang, C.T. Chan, and K.M. Ho, Phys. Rev. B **45**, 12 227 (1992).
[17] A.P. Horsfield and P. Clancy, Model. Simul. Mater. Sci. Eng. **2**, 277 (1994).
[18] L. Colombo and G. Servalli, *Materials Theory and Modelling*,

edited by P.D. Bristowe *et al.* (Materials Research Society, Pittsburgh, 1993).
[19] C.H. Xu, C.Z. Wang, C.T. Chan, and K.M. Ho, J. Phys. Condens. Matter **4**, 6047 (1992).
[20] C.Z. Wang and K.M. Ho, Phys. Rev. B **50**, 12 429 (1994).
[21] F. Ducastelle and F. Cyrot-Lackmann, J. Phys. Chem. Solids **31**, 1295 (1970).
[22] R. Haydock, Solid State Phys. **35**, 216 (1980).
[23] D.G. Pettifor, Phys. Rev. Lett. **63**, 2480 (1989).
[24] M. Aoki, Phys. Rev. Lett. **71**, 3842 (1993).
[25] S. Goedecker and L. Colombo, Phys. Rev. Lett. **73**, 122 (1994).
[26] J.D. Kress and A.F. Voter, Phys. Rev. B **52**, 8766 (1995).
[27] V. Heine, Solid State Phys. **35**, 1 (1980).
[28] C. Lanczos, J. Res. Natl. Bur. Stand. **45**, 225 (1950).
[29] N. Beer and D.G. Pettifor, *Structure and Phase Stability of Alloys*, edited by P. Phariseau and W. Temmerman (Plenum Press, New York, 1984).
[30] M.W. Finnis and J.E. Sinclair, Philos. Mag. A **50**, 45 (1984).
[31] R. Jones and M.W. Lewis, Philos. Mag. B **49**, 95 (1984).
[32] J. Inoue and Y. Ohta, J. Phys. C **20**, 1947 (1987).
[33] A.T. Paxton, A.P. Sutton, and C.M.M. Nex, J. Phys. C **20**, L263 (1987).
[34] A.T. Paxton and A.P. Sutton, Acta Metall. **37**, 1693 (1989).
[35] A.A. Abrikosov, L.P. Gorkov, and I.E. Dzyaloshinski, *Methods of Quantum Field Theory in Statistical Physics* (Prenctice-Hall, Englewood Cliffs, NJ, 1963).
[36] G. Allan, M.C. Desjonqueres, and D. Spanjaard, Solid State Commun. **50**, 401 (1984).
[37] P. Turchi, F. Ducastelle, and G. Tréglia, J. Phys. C **15**, 2891 (1982).